Low-temperature crystallization of high performance Pb0.4Sr 0.6TiO3 films compatible with the current silicon-based microelectronic technology

K. Li, Denis Remiens, X.L. Dong, J. Costecalde, N. Sama, T. Li, G. Du, Y. Chen, G.S. Wang

Applied Physics Letters

Low-temperature crystallization of high performance $Pb_{0.4}Sr_{0.6}TiO_3$ films compatible with the current silicon-based microelectronic technology

Cite as: Appl. Phys. Lett. **102**, 212901 (2013); https://doi.org/10.1063/1.4807792
Submitted: 23 January 2013 • Accepted: 11 May 2013 • Published Online: 28 May 2013

Kui Li, Denis Rémiens, Xianlin Dong, et al.

AIP Publishing

Low-temperature crystallization of high performance $Pb_{0.4}Sr_{0.6}TiO_3$ films compatible with the current silicon-based microelectronic technology

Kui Li,[1] Denis Rémiens,[2] Xianlin Dong,[1] Jean Costecalde,[2] Nossikpendou Sama,[2] Tao Li,[1] Gang Du,[1] Ying Chen,[1] and Genshui Wang[1,a)]

[1]*Key Laboratory of Inorganic Functional Materials and Devices, Shanghai Institute of Ceramics, Chinese Academy of Sciences, 1295 Dingxi Road, Shanghai 200050, People's Republic of China*
[2]*Institute of Electronics, Microelectronics and Nanotechnology (IEMN) DOAE, UMR CNRS 8520, Université des Sciences et Technologies de Lille, 59652, Villeneuve d'Ascq Cedex, France*

(Received 23 January 2013; accepted 11 May 2013; published online 28 May 2013)

This investigation presents a simple approach to realize the low temperature crystallization of $Pb_{0.4}Sr_{0.6}TiO_3$ thin films at 400 °C by taking advantage of well controlled lead excess and kinetic-driving-force compensated thermodynamics crystalline via sputtering deposition. The thin films prepared at low temperature show fine-grained micro-structure because of the suppressed grain growth, furthermore, the intrinsic dielectric response can be modulated by the distinct level of crystallinity. The film processed at 450 °C exhibited a dielectric constant of 435 and high figure merit of 130 at 400 kV/cm, superior ferroelectric property, and stable performance with temperature and frequency. © *2013 AIP Publishing LLC*. [http://dx.doi.org/10.1063/1.4807792]

Ferroelectric thin films integrated with silicon-based semiconductor are of great interest for a wide array of applications in wireless microwave communication devices and ferroelectric random access memories because of their excellent tunable and ferroelectric properties.[1–3] The integration of the ferroelectric thin films onto the silicon-based semiconductor is a critical issue for the device applications, which requires low-temperature (<500 °C) processing due to the probable damage of devices and interconnection fabricated on silicon semiconductor substrates at high temperature.[4] Moreover, the high processing temperature also favors the inter-diffusion between the thin film and the bottom electrode, thus causing the deterioration of the electrical properties.[5] Lead Strontium Titanate (PST) thin film is one of the most promising candidate materials for the applications mentioned above owing to its excellent properties and much lower processing temperature in comparison to the extensively studied $Ba_{1-x}Sr_xTiO_3$ (BST) thin film.[6] Hitherto, various approaches have been adopted to reduce the perovskite crystallization temperature of the ferroelectric films with good performance and relatively successes have been achieved by microwave heating crystallization at 450 °C,[7] localized heating via pulsed laser at low temperatures of 350–400 °C (Ref. 8), and on axis RF-magnetron sputtering at 500 °C (possessing very poor performance at 450 °C).[9] Nevertheless, microwave heating results in damage of silicon-based circuits, the costly pulsed laser processing is unfavorable for industrial application, while the on axis RF-magnetron sputtering provides insufficient film quality at low temperature.

Moreover, as the continuous miniaturization of current microelectronics device size and the shrinking dimension of the ultra-large-scale integrated (ULSI) circuits, the contradiction between the demand for the fine-grained ferroelectric thin films and the attenuate dielectric and ferroelectric properties in these films becomes the major factor limiting the practical applications of these films. It is thus critically important to prepare ferroelectric thin films with small volumes and investigate the effect of grain size on the properties. There are very few associated investigations on the effect of grain size on the properties of PST thin films due to the lack of effective methods to prepare the fine-grained films.

Regarding the frequency agile applications, the researchers normally improved the tunability by increasing the dielectric constant under zero electric field because the dielectric response under the maximum electric field is mainly contributed by the intrinsic dielectric response (related to lattice deformation) and nearly constant for the dense and well crystallized perovskite films.[9–11] However, the higher dielectric constant is in the cost of higher loss tangent and may cause some integration problems.[12] Unfortunately, there are very rare reports on the modulation of dielectric response under the maximum electric field to obtain better tunable performance.

The central object of the present work is to realize the low temperature crystallization while maintain the fairly good performance of $(Pb_{0.4}Sr_{0.6})TiO_3$ thin films by taking advantage of the favorable lead excess and kinetics improved crystallization through optimizing the annealing periods. PST films with fine-grained micro-structure were prepared via suppressing the grain growth. Moreover, the dielectric constant under the maximum electric field is modulated by controlling the degree of crystallinity stemming from the low annealing temperature to obtain better tunablility performance.

$Pb_{0.4}Sr_{0.6}TiO_3$ ceramic with 25 wt. % lead excess and 6 wt. % strontium excess was used as target. The perfect (100)-oriented $Pb_{0.4}Sr_{0.6}TiO_3$ thin films with a thickness of 400 nm were deposited with off-axis RF-magnetron sputtering method without heating the substrate on the (100) $LaNiO_3$ bottom electrode.[13] The substrate was tilted 25° from the normal direction to the target surface. The total gas pressure during deposition was 30 mTorr in an atmosphere of pure Ar, and the RF power was kept at 60 W. The as deposited PST thin films were transformed to a crystalline

a)Electronic mail: genshuiwang@mail.sic.ac.cn

phase through a post annealing process. To compensate effect of the insufficient thermodynamics energy, longer annealing periods representing the kinetic driving force were adopted for the films post-annealed at low temperature. The Pt top electrode with a diameter of 150 μm was prepared with the traditional photolithography and lift-off processes. X-ray diffraction (XRD) analysis (Siemens D5000 diffractometer) and scanning electronic microscope (SEM) Hitachi S4800 (Hitachi, United State of America, TX) were adopted to investigate the crystal quality and micro-structure of the PST thin films. The dielectric constant and loss tangent dependences on the electric field were tested by HP4192A LCR meter under ac voltage of 0.1 V with the frequency of 10 kHz.

Fig. 1(a) shows the XRD patterns for the PST thin films post-annealed at temperatures ranging from 400 to 650 °C (abbreviated as PST-400 to PST-650). The initial crystallization temperature is 500 °C for the films annealed for 1 h, while the films are crystallized at a temperature as low as 400 °C with longer annealing periods, which may be attributed to the kinetics energy compensation for the insufficient thermodynamics energy at lower post-annealing temperature. The crystallization process can be assumed to be the combined impacts of the thermodynamics and kinetics driving force. The films may be first transformed into the metastable state, which is characterized by the transient nucleus and the low level of the rate of formation of nuclei. During the process of translation from this transient state to the crystallized steady-state, the metastable nucleus captures atoms and develops to the steady-nucleus; meanwhile, the rate of the formation of nuclei increases to the critical number. The number of the steady nuclei per unit volume increases with time and eventually saturates at the constant value.[14] For the thin films post-annealed at low temperature, the critical nucleus can capture more atoms easily to form the critical nucleus and then the steady nuclei with longer periods, and it will cost longer time to reach the critical rate of formation of nuclei because of much lower diffusion activation and adsorption energy for lower post-annealing temperature. However, the films post-annealed at 350 °C show amorphous phase even for a longer annealing period of 24 h, indicating a threshold thermodynamics energy for the formation of the metastable phase, below which even longer post-annealing periods can not induce the crystallization of the films. The post-annealing periods were optimized to increase the properties and density of the thin films, for example, PST-450 for 8 h and PST-400 for 12 h. The Inductively Coupled Plasma (Aglient, America, Vista AX) was adopted to compare the stoichiometry composition for the films prepared with on and off axis deposition (not shown here). The results reveal that the Pb/(Pb + Sr) of the films prepared with off-axis deposition is 0.47 and decreases to 0.37 for those with on-axis deposition.[9] It should be paid close attention that the amount of (Pb + Sr) is larger than that of Ti for the on and off-axis deposition. The excess of PbO may enhance the mobility of the ions and promote the formation of crystalline structure at lower processing temperature[15] and suppress the formation of pyrochlore phase consequently decrease the crystallization temperature.[16] Moreover, growth speed of off axis deposition is much lower than that of on axis one,[9] which may favor the epitaxial growth of the films on bottom electrode.

The scanning electronic microscope photos were demonstrated in parts (b)-(d) in Fig. 1. All the films ranging from PST-400 to PST-650 exhibit dense and crack-free microstructure and obvious grain structure. However, the grain size decreases dramatically with decreasing post-annealing temperature even for longer post-annealing periods. The longer annealing periods just improves densification but not favors the growth of the grain. The densification needs lower driving force[17] than that of grain growth and the initial temperature for the grain growth may be higher than 450 °C, thus the films post-annealed at 450 and 400 °C just show increasing density while little grain growth, which is of industrial importance in fabricating the fine-grained ferroelectric thin films.

The electric field dependence of the polarization hysteresis (P–E) loops of PST-650 and PST-450 were measured using an aixACCT TF Analyzer 2000 system with frequency of 1000 Hz. As demonstrated in Fig. 2, the PST-650 shows advantageous ferroelectric properties: $P_r = 4.9\ \mu C/cm^2$ and $E_c = 48$ kV/cm at an electric field of 400 kV/cm. Interestingly, the ferroelectric property did not decrease dramatically with

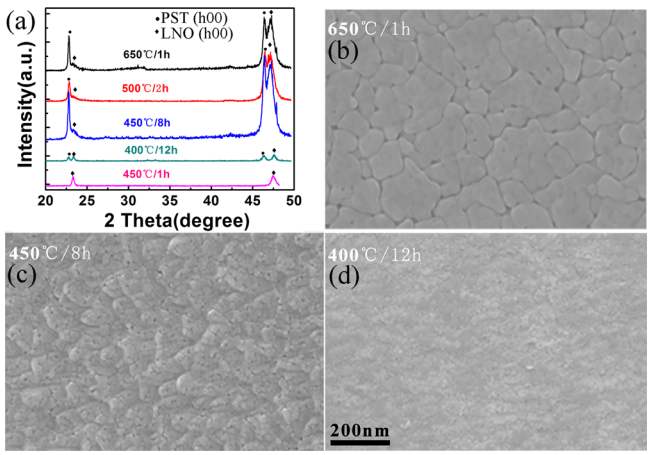

FIG. 1. The (a) X-ray diffraction patterns and scanning electron microscope (SEM) photographs of PST films post-annealed at (b) 650 °C, (c) 450 °C, and (d) 400 °C.

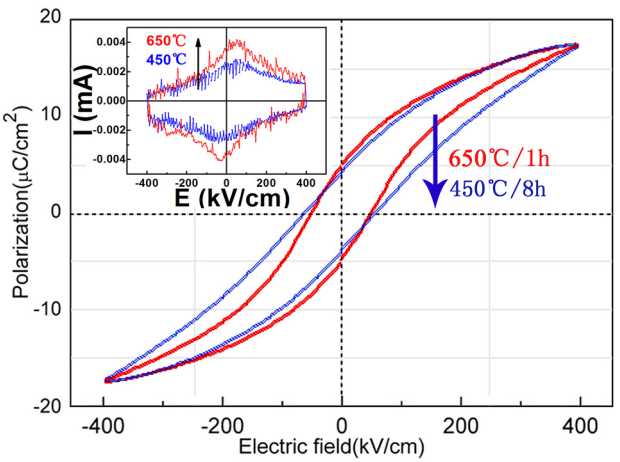

FIG. 2. Ferroelectric responses (P-E loops) of the PST thin films annealed at 450 and 650 °C. Inset shows the current—electric field loops of the films prepared at 450 and 650 °C.

the decreasing post-annealing temperature and grain size. The PST-450 shows P_r and E_c of 4.2 μC/cm^2 and 57.5 kV/cm, respectively, indicating that the fine-grained PST films maintain fairly good ferroelectric properties. To make the effect of post-annealing temperature on the ferroelectric property of PST thin film more clearly, the current-electric field loops were displayed as inset in Fig. 2. It can be found that the maximum current corresponding to the domain switching peaks appear near the coercive field[18] and the peaks become a little stronger with higher post-annealing temperature. Moreover, the much narrower current peak near coercive field for PST-650 in comparison with that of PST-450 indicates that mass domain switches in a shorter time, which explains the much larger gradient in the sloop of PST-650 near E_c.

Fig. 3 demonstrates the dielectric constant and loss tangent of PST films annealed at different temperature as a function of DC electric field. It is observed that the relative permittivity under zero electric field increases gradually with the post-annealing temperature increasing from 400 to 650 °C because of the improved the crystallization of the films. Fortunately, the thin films with much smaller grain size because of the lower annealing temperature show favorable dielectric constant (435 for PST-450 and 387 for PST-400, respectively) in comparison to that of PST-500. However, the dielectric constant under the maximum electric field first increases dramatically from PST-400 to PST-500 and then maintains a stable value with the post-annealing temperature increasing further to 650 °C. This difference is the result of the different evolution of intrinsic and extrinsic relative permittivity dependence on the DC electric field. Normally, the extrinsic dielectric response is dominated by the domain wall motion, while the intrinsic dielectric response is related to the lattice deformation.[19] The former will be suppressed by the high DC electric field because the movement of domain is not easy under high electric field.[10] The modulated intrinsic dielectric response under the maximum electric field favors the better tunable performance of the films prepared with lower temperature. Interestingly, the much smaller grain size of the films annealed at 450 °C increase the number of grain boundary, which is favorable for the better loss tangent performance because of the lower level of interface diffusion as reported for $Ba(Ti_{0.85}Sn_{0.15})O_3$ films[20] and suppressed charged carrier. The PST-400 shows a relative high loss tangent because of its poor crystallization. As shown in the inset, the PST-450 shows weak dielectric response depression (line (a)) which represents the uniformity of the composition and crystallization with the frequency increasing from 100 Hz to 1 MHz and relatively good dielectric constant (line (b)) and loss tangent stability with temperature, suggesting that the films prepared at low temperature can be used in wider conditions without a dramatic variation of properties.

The evolution of relative permittivity and tunability dependence on DC electric field are calculated and displayed in Fig. 4. The tunability and the figure of merit (abbreviated as FOM) are defined as

$$\eta = \{[\varepsilon(0) - \varepsilon(E_{\max})]/\varepsilon(0)\} \times 100\%, \quad (1)$$

$$FOM = \frac{\eta}{\tan\delta}, \quad (2)$$

where the $\varepsilon(0)$ and $\varepsilon(E_{\max})$ are the relative permittivity under zero and the maximum DC electric field, respectively. The $\varepsilon(0)$ is mainly contributed by the extrinsic dielectric response and increases gradually from PST-400 to PST-650 (387 for PST-400 and 605 for PST-650, respectively), while the $\varepsilon(E_{\max})$, mainly contributed by the intrinsic dielectric response stemming from the lattice deformation, first increases from PST-400 to PST-500 and then keeps a constant value of 191 to PST-650 because of the similar intrinsic dielectric response for the films with complete crystallization. Interestingly, the low intrinsic response for the films prepared at low temperature favors the better tunability of PST-400 (66.8%) and PST-450 (65%), which are outstanding in comparison with that of the PST thin films processed at 500 °C reported by the Lei[9] under an electric field of 400 kV/cm. Moreover, the films annealed at lower temperature show much higher FOM (130 for PST-450) than those annealed at higher temperature in this work (23 for PST-650) and the result reported by Lei (30 for the films prepared at 650 °C)[9] because of its much lower loss tangent.

In summary, by taking advantage of the favorable lead excess and kinetic driving force-compensated thermodynamics crystalline, the device-quality $Pb_{0.4}Sr_{0.6}TiO_3$ thin films

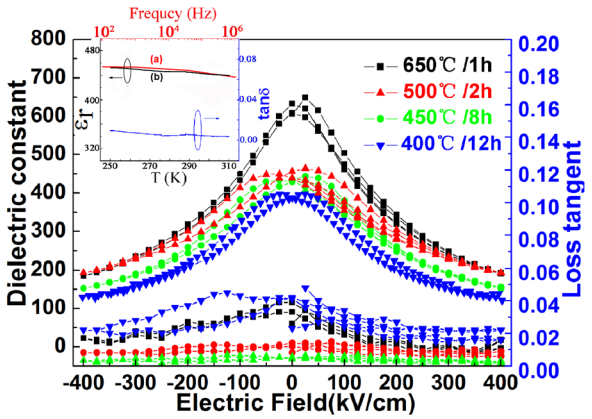

FIG. 3. The dielectric constant and the loss tangent of PST thin films annealed at different temperature as a function of DC bias field. Inset shows the dielectric constant (ε_r)—frequency evolution (line (a)) and dielectric constant (line (b)) as well as loss tangent versus temperature of the film post-annealed at 450 °C.

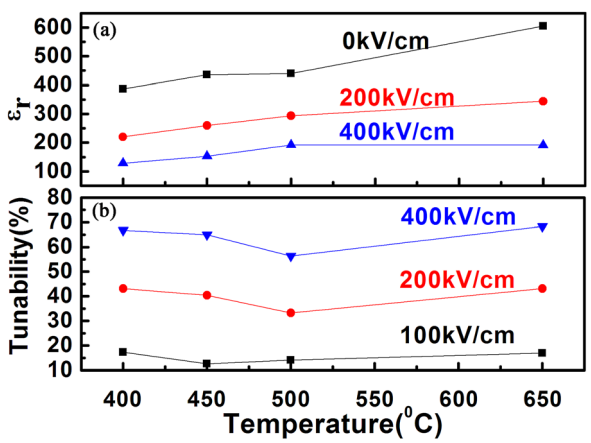

FIG. 4. The effect of annealing temperature on the (a) dielectric constant (ε_r) and (b) tunability of the PST films.

crystallized at 400 °C were realized via the off axis RF-magnetron sputtering. The micro-structure analysis indicates that the thin films prepared with low temperature show fine-grained while dense structure, stemming from the suppressed grain growth, and distinct degree of crystallization. The electrical measurement results indicate that the PST films prepared at 450 °C exhibited high tunable performance, superior ferroelectric property, and stable performance with temperature and frequency, making potential applications in frequency agile devices compatible with the current Si integrated circuit technology.

This work was supported by Key Basic Research Project (973 Program) (Grant No. 2012CB619406), the National Natural Science Foundation of China (No. 10974216 U0937603), and Open Project Key Laboratory of Polar Materials and Devices, Ministry of Education (Grant No. KFKT20120001).

[1]D. Dimos and C. H. Mueller, Annu. Rev. Mater. Sci. **28**, 397 (1998).
[2]O. Lee, S. A. Harrington, A. Kursumovic, E. Defay, H. Y. Wang, Z. X. Bi, C. F. Tsai, L. Yan, Q. X. Jia, and J. L. MacManus-Driscoll, Nano Lett. **12**, 4311 (2012).
[3]M. Jain, N. K. Karan, R. S. Katiyar, A. S. Bhalla, F. A. Miranda, and F. W. Van Keuls, Appl. Phys. Lett. **85**, 275 (2004).
[4]M. L. Calzada, I. Bretos, R. Jimenez, H. Guillon, and L. Pardo, Adv. Mater. **16**, 1620 (2004).
[5]Q. G. Chi, X. Wang, W. L. Li, W. D. Fei, and Q. Q. Lei, Appl. Phys. Lett. **98**, 242903 (2011).
[6]M. Liu, C. R. Ma, G. Collins, J. A. Liu, C. L. Chen, L. Shui, H. Wang, C. Dai, Y. A. Lin, J. He, J. C. Jiang, E. I. Meletis, and Q. Y. Zhang, Cryst. Growth Des. **10**, 4221 (2010).
[7]Z. J. Wang, H. Kokawa, H. Takizawa, M. Ichiki, and R. Maeda, Appl. Phys. Lett. **86**, 212903 (2005).
[8]J. L. Wang, Y. S. Lai, B. S. Chiou, C. C. Chou, T. G. Y. Lee, H. Y. Tseng, C. K. Jan, and H. C. Cheng, Appl. Phys. A **90**, 129 (2008).
[9]X. Y. Lei, D. Remiens, F. Ponchel, C. Soyer, G. S. Wang, and X. L. Dong, J. Am. Ceram. Soc. **94**, 4323 (2011).
[10]C. Ang and Z. Yu, Appl. Phys. Lett. **85**, 3821 (2004).
[11]L. Yang, G. Wang, X. Dong and D. Remiens, J. Am. Ceram. Soc. **93**, 350 (2010).
[12]A. B. Kozyrev, A. D. Kanareykin, E. A. Nenasheva, V. N. Osadchy, and D. M. Kosmin, Appl. Phys. Lett. **95**, 012908 (2009).
[13]L. Yang, G. Wang, C. Mao, Y. Zhang, R. Liang, C. Soyer, D. Remiens, and X. Dong, J. Cryst. Growth **311**, 4241 (2009).
[14]M. Ohring, *Materials Science of Thin Films: Deposition and Structure*, 2nd ed. (Academic Press, San Diego, CA, 2002).
[15]I. Bretos, R. Jimenez, J. Garcia-Lopez, L. Pardo, and M. L. Calzada, Chem. Mater. **20**, 5731 (2008).
[16]J. W. Li, H. Kameda, B. N. Q. Trinh, T. Miyasako, P. T. Tue, E. Tokumitsu, T. Mitani, and T. Shimoda, Appl. Phys. Lett. **97**, 102905 (2010).
[17]I. W. Chen and X. H. Wang, Nature **404**, 168 (2000).
[18]H. X. Yan, F. Inam, G. Viola, H. P. Ning, H. T. Zhang, Q. H. Jiang, T. Zeng, Z. P. Gao, and M. J. Reece, J. Adv. Dielectr. **1**, 107 (2011).
[19]Q. M. Zhang, H. Wang, N. Kim, and L. E. Cross, J. Appl. Phys. **75**, 454 (1994).
[20]S. J. Wang, S. Miao, I. M. Reaney, M. O. Lai, and L. Lu, Appl. Phys. Lett. **96**, 082901 (2010).